

Supplemental Materials

Combining ATR suppression with oncogenic Ras synergistically increases genomic instability, causing synthetic lethality or tumorigenesis in a dosage-dependent manner

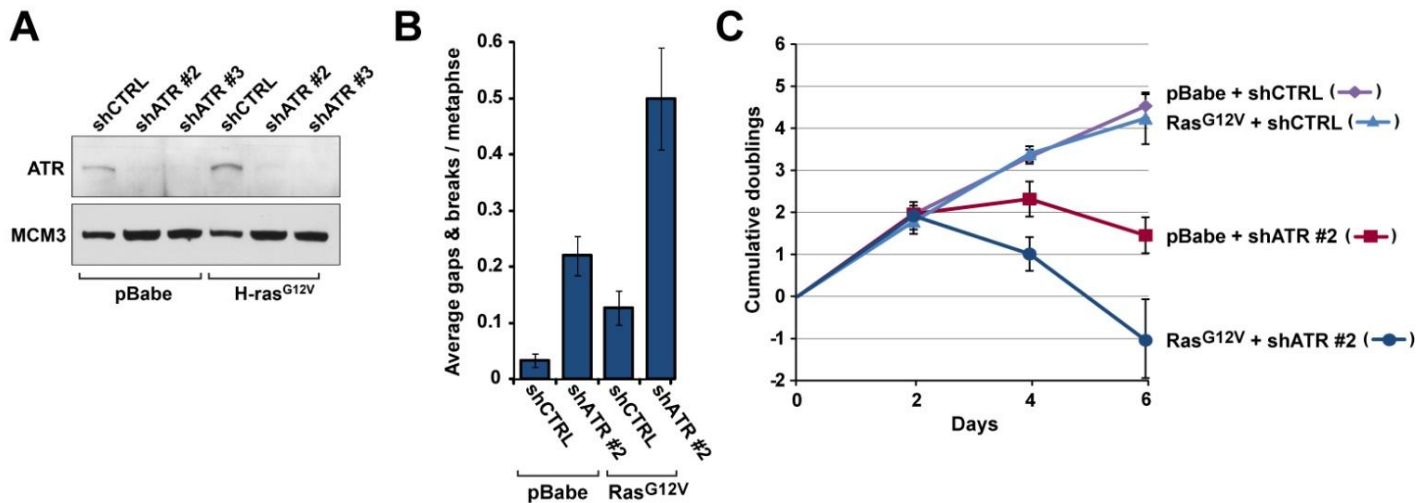
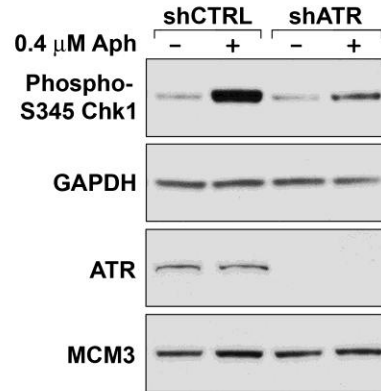
Oren Gilad¹, Barzin Y. Nabet¹, Ryan L. Ragland¹, David W. Schoppy¹, Kevin D. Smith¹, Amy C. Durham² and Eric J. Brown^{1*}

¹Abramson Family Cancer Research Institute and the Department of Cancer Biology, University of Pennsylvania School of Medicine and ²School of Veterinary Medicine, Philadelphia, PA 19104.

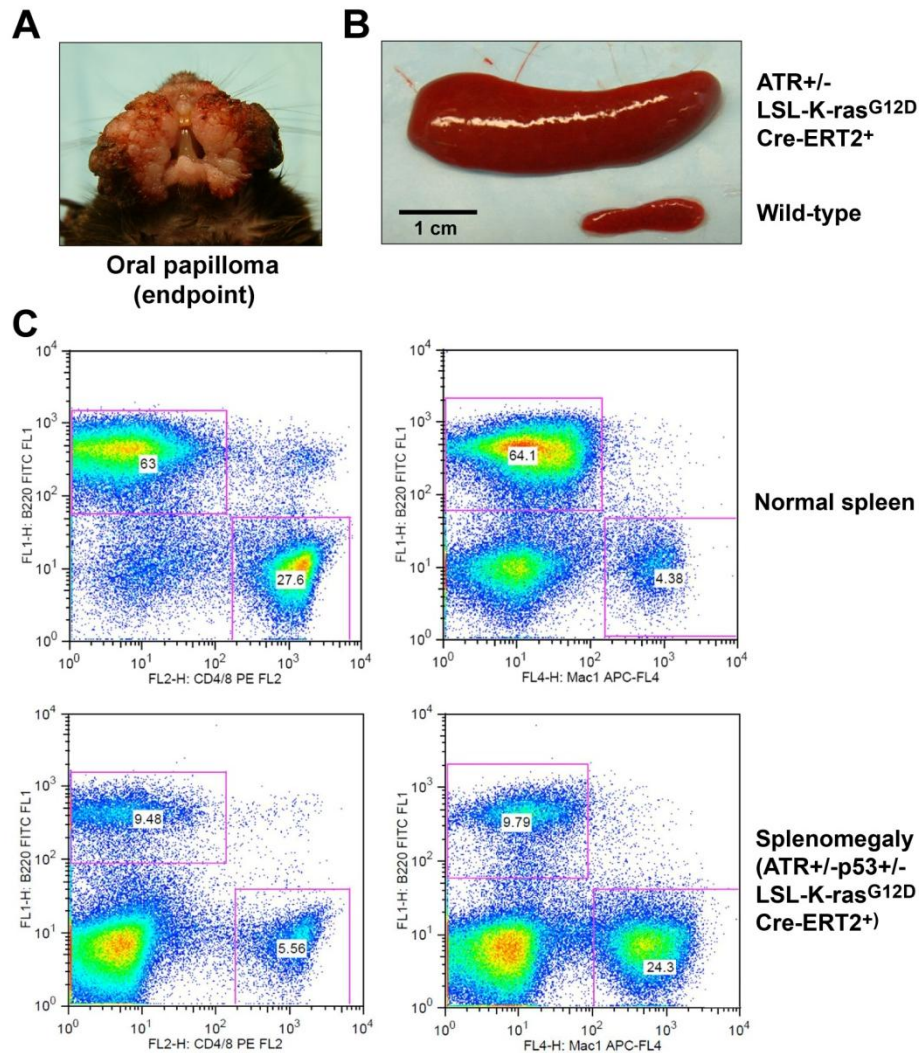
*To whom correspondence should be addressed:

Eric J. Brown, Abramson Family Cancer Research Institute and the Department of Cancer Biology, University of Pennsylvania School of Medicine, 421 Curie Boulevard, Philadelphia, PA 19104. Phone: 215-746-2805; Fax: 215-573-2486; E-mail: brownej@mail.med.upenn.edu

Supplemental Figure 1. Hypomorphic ATR suppression is sufficient to limit aphidicolin-induced phosphorylation of Chk1 on S345. ATR expression was reduced by shRNA-mediated targeting in H-ras^{G12V}-transformed NIH3T3 cells, as performed for experiments shown in Figs. 2 and 3 and described in *Materials and Methods*. Aphidicolin (Aph) was added for 1 hour prior to harvest and whole cell lysates were detected for phospho-S345 Chk1 and ATR as shown. GAPDH and MCM3 were detected as protein loading controls for Chk1 and ATR, respectively.

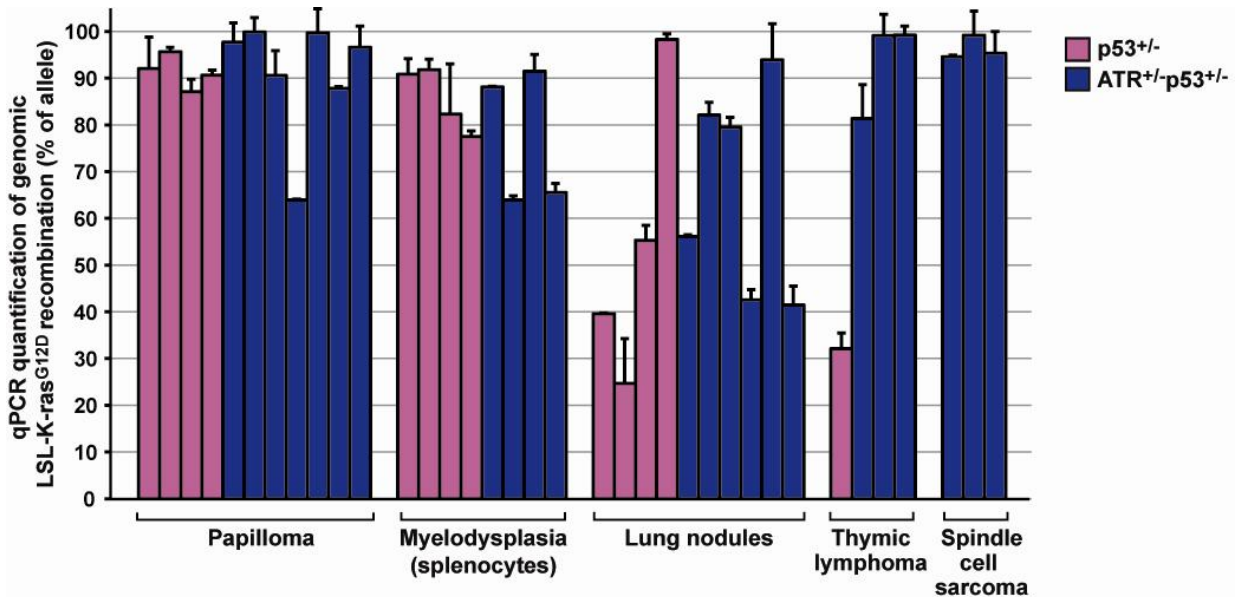
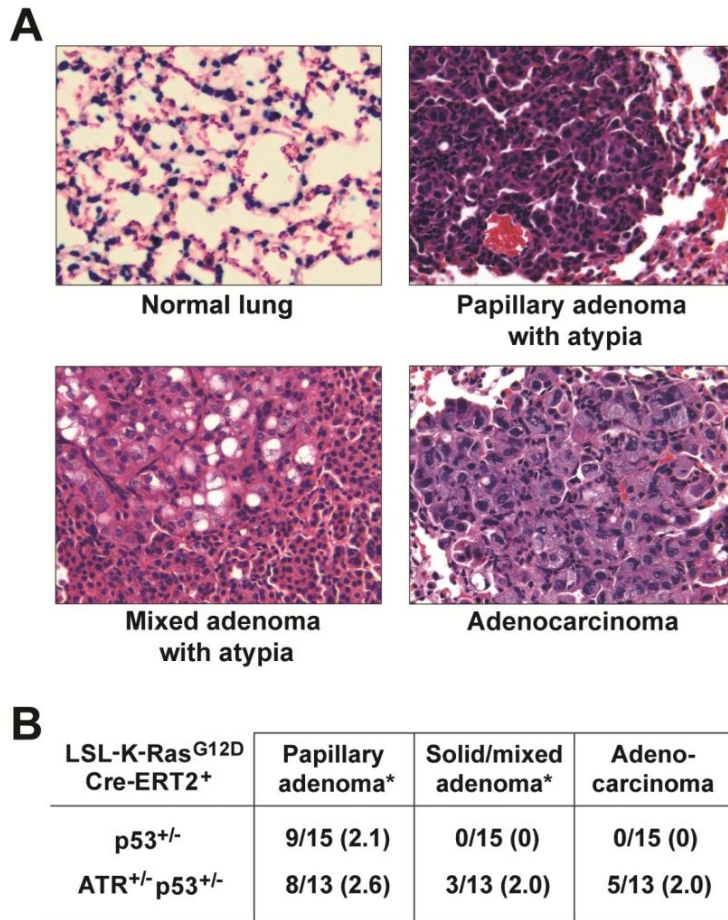


Supplemental Figure 2. ATR suppression using additional distinct shRNAs elevates genomic instability and causes synthetic lethality when combined with H-ras^{G12V} transformation. **A**, Independent shRNA-mediated reduction of ATR expression. Suppression of ATR protein levels by expression of additional shRNAs specific for murine ATR (shATR #2, TRC23910 and shATR #3, TRC23911) was determined by western blot. ShRNA expression was driven from integrated lentivirus (pLKO), produced as described in *Material and Methods*. MCM3 was detected as a loading control. **B**, Quantification of chromatid breaks. ATR expression was reduced in control and H-ras^{G12V}-transformed cells, and mitotic spreads were analyzed for chromatid breaks as described in *Material and Methods* and Fig. 2. **C**, Effect of independent shRNA-mediated ATR suppression on the proliferation of control and H-ras^{G12V}-transformed cells was performed as described in *Material and Methods* and Fig. 3. Negative numbers indicate the calculated cumulative loss (log₂) compared to initial plating at time 0.



Supplemental Figure 3. Highly penetrant mouth papilloma and myeloproliferation following K-ras^{G12D} expression. A, Gross pathology of oral papillomas observed in tamoxifen-treated LSL-K-ras^{G12D} mice. B, Splenomegaly in mice conditionally expressing K-ras^{G12D}. Representative examples of spleens from wild-type (bottom) and tamoxifen-treated LSL-K-ras^{G12D} (top) mice. The ATR^{+/-}LSL-K-ras^{G12D} spleen shown was isolated 52 days after low-dose tamoxifen treatment. C, Flow cytometric analysis of splenocytes isolated from control (Cre-ERT2-negative) and low-dose tamoxifen-treated ATR^{+/-}p53^{+/-}LSL-K-ras^{G12D} mice. Splenocytes were stained with antibodies recognizing CD4 and CD8, Mac1 and B220 and detected populations were gated and quantified as indicated. The percentage of gated cells demonstrates a proportional reduction in B and T cell lineages and an enrichment of Mac1⁺ and Mac1⁻ cell types in tamoxifen-treated LSL-K-ras^{G12D} mice. These characteristics are similar to the previously reported myeloproliferative effects of K-ras^{G12D} expression in the bone marrow (44, 46).

Supplemental Figure 4. ATR haploinsufficiency synergizes with K-ras^{G12D} expression to promote the generation of lung adenoma and adenocarcinoma. A, Representative histopathology of observed lesions in sectioned lungs. Solid/mixed adenoma with atypia and lung adenocarcinoma were observed exclusively in tamoxifen-treated ATR^{+/-}p53^{+/-}LSL-K-ras^{G12D/+}Cre-ERT2⁺ mice. Tumor classification was performed as described (32). Normal lung section shown was isolated from a p53^{+/-} control mouse. B, Number of animals affected with select lung pathologies. The average number of tumors observed per lung of affected animals is indicated in parentheses. Asterisks indicate adenomas with atypical features.



Supplemental Figure 5. Quantification of lox recombination of the LSL-K-ras^{G12D} allele in isolated tumors. Real-time quantitative PCR (qPCR) analyses of genomic DNA isolated from tumors are displayed in the same order as that shown in Fig. 5B. Standard errors (bars) were calculated from three or more independent PCR reactions. qPCR analysis was performed as described in Fig. 4B and *Materials and Methods*.